ASSESSING IMPACT OF ECONOMIC ACTIVITIES ON URBAN AIR QUALITY IN INDIA BY NIGHTLIGHT AND ATMOSPHERIC MEASUREMENT DATASETS

Prakhar Misra & Wataru Takeuchi

Institute of Industrial Science, The University of Tokyo, Meguro 4-6-1, Tokyo 153-8505, Japan

E-mail:mprakhar@iis.u-tokyo.ac.jp

KEYWORDS: calibration, Granger causality, GDP

ABSTRACT: Understanding causal relationship between economic activities and emissions is important for framing successful environmental policies. However temporally and spatially continuous 'air quality' data is required to get a detailed trend information for urban regions. Using nightlight data, which correlate well with economic activities, and air quality species data observed from satellite, the authors have previously devised a scheme for classifying regions. In this research the classification scheme is applied on a time series data to draw inferences about transition in regional air quality due to human activities. Based on inferences from classification trends, relationship between various economic activities (such as construction, manufacturing, vehicle population etc.) and air quality species is explored and checked for causality using Granger's test. The objective is to identify which industries correlate well with air quality species and can also be statistically identified as a cause.The air quality species considered are ANG (angstrom exponent), AOD (aerosol optical depth), NO_2, SO_2 Nightlight time series data is obtained by intra-calibrating DN values from multiple-year DMSP-OLS sensors and inter-calibrating it with radiance values from VIIRS-DNB sensor. The industries that are expected to result in nighttime lights and urban air pollution are then checked for causality with air quality species using Granger causation test.

1 INTRODUCTION

1.1 Background

Understanding causal relationship between economic activities and emissions is important for framing successful environmental policies. Therefore, the role of economic activities promoting anthropogenic pollutants needs to be confirmed before implementing corrective policies. However to get a detailed trend information for urban regions, temporally and spatially continuous data is required. Previously Fujikawa and Takeuchi (2013) used remote sensing MODIS and OMI data to characterize air quality of multiple urban regions globally with regards to their gross domestic product (GDP) where it was found that with increasing GDP of cities the air pollution levels first rose drastically and then fell down gradually. This Environmental Kuznets Curve (EKC) type relationship has also been found for the Indian case while studying relationship of environmental productivity and income (Managi and Jena, 2008) and carbon emissions and economic activity (Kanjilal and Ghosh, 2013). High correlations of nightlight with gross domestic product (GDP) (0.88) and motor-vehicle count(0.91) have been reported at country level by Katayama and Takeuchi (2014) on a global scale highlighting its utility in representing regions with socio-economic activities.

In recent years Indian cities have seen a worsening trend of air quality (Misra and Takeuchi, 2015). By considering this information as per the EKC, a question arises if this is a result of robust economic growth in India. It therefore becomes necessary to find which economic sectors correlate well with urban air quality. It is further necessary to find if the economic sectors so identified are also the cause of poor urban air quality. As per United Nations urban regions are defined in terms of administrative boundary, population size, economic function and built-up characteristics. However in the present study urban regions are considered as regions that can be captured using night light.

1.2 Objective

The objective of this research is to identify those economic sectors whose annual GDP correlates well with urban air quality and to probe the nature of causality for such relationships.

2 DATA AND METHODOLOGY

2.1 Datasets

This study used records from the year 2004 to 2014 from three types of datasets: air-quality, nighttime light and macroeconomic domestic productivity.

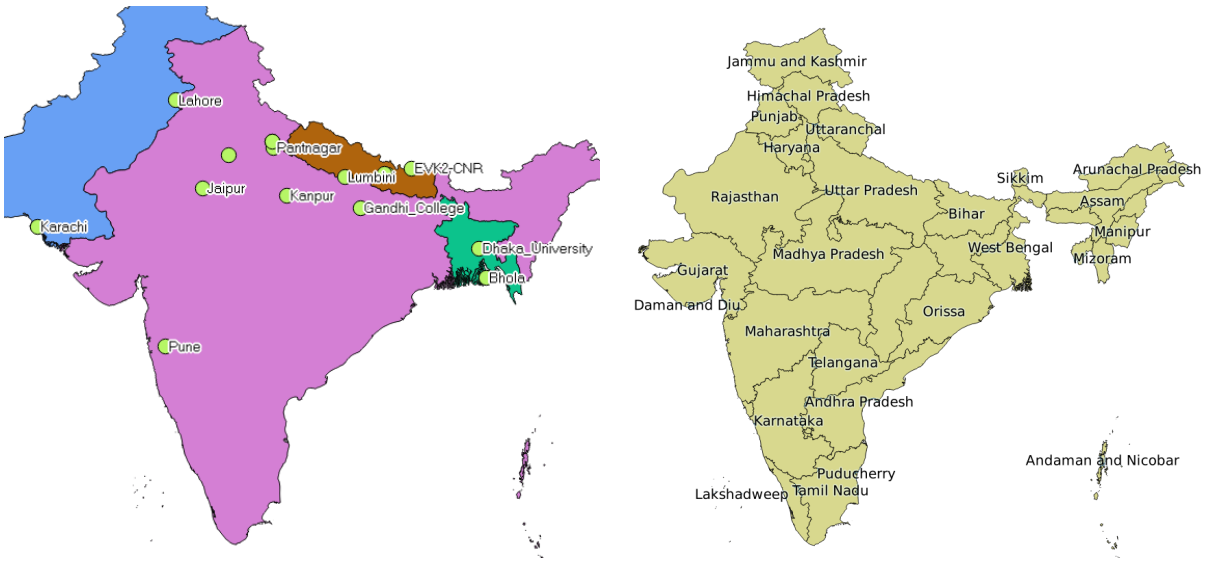

(a) (b)

Figure 1: (a) Location of AERONET stations considered. India is shown is magenta color. (b) The states and union territories in India

Air-quality datasets (AQ): The air-quality species considered were ANG, AOD, SO_2 and NO_2 (collectively referred to as AQ in henceforth). To study ANG and AOD levels, daily 'MOD04L2' Level-2 data at 10km resolution obtained from Moderate Resolution Imaging Spectroradiometer (MODIS) sensor onboard NASA's EOS Terra satellite was used. 'Deep_Blue_Aerosol_Optical_Depth_ 550_Land' dataset was used for AOD images and 'Deep_Blue_Angstrom_ Exponent_Land' dataset was used for ANG images. To study SO_2 and NO_2 column concentration levels for June 2014, 'OMSO2e' and 'OMNO2d' Level-3 Ozone Monitoring Instrument (OMI) daily datasets from NASA's EOS Aura were used respectively. This data has a spatial resolution of approximately 25km. In addition AOD data from 14 of the AERONET stations (shown in Figure 1a) , a global network of ground based sun-photometers (Holben et al., 1998), in the Indian subcontinent having more than 280 days of measurement were used to check the reliability of MODIS derived AOD estimates.

Nighttime Light (NL): For the years 2004 to 2013, annual stable nighttime light composites at approximately 2.7km spatial resolution from the OLS (Operational Linescan System) sensor aboard DMSP (Defense Meteorological Satellite Program) were used. For some years composites from multiple DMSP-OLS satellites are also available yet composites only from satellites F16 and F18 were considered. This was done to avoid as much inter-calibration errors as possible due to lack of on-board calibration system (Elvidge et al., 2009). Since the OLS dataset is publicly available only until 2013, day-night band (DNB) product (Baugh et al., 2013) of Visible Infrared Imaging Radiometer Suite (VIIRS) dataset for the years 2013 and 2014 was used. Its spatial resolution is approximately 0.75km. DNB provides surface radiance values in contrast to 6-bit quantization of OLS, which is a digital number (DN) based product with values ranging from 0 to 63. These datasets are provided by National Oceanic and Atmospheric Administration's (NOAA) National Geographic Data Center (NGDC).

Gross domestic product (GDP): For India, GDP information is publicly available (*https://data.gov.in/*) at administrative resolution of country, state (or province as in other countries) and districts. Country and state (numbering 28 except the state of Telangana) level data is available by sectoral composition of the GDP (Central Statistic Office, 2012) for years 2004-2014. The states are shown in Figure 1b. The overall GDP was only found available for 160 districts (out of the total 640 districts) for years 2004-2011. The sectoral composition structure is shown in Table1

2.2 Flowchart

Figure 2 lays down the flowchart of data processing and analysis performed to obtain results.

Table 1: Structural composition of GDP in India by economic sectors.

Ag & Allied (Primary)	Industry (Secondary)	Services (Tertiary)
Agriculture &	Mining & quarrying	Transport
Forestry & logging	Registered Manufacturing	Storage
Fishing	Unregistered Manufacturing	Communication
	Construction	Railways
	Electricity, gas & Water supply	Banking & Insurance
		Real estate, ownership of dwellings & business services
		Public Administration
		Trade, hotels & restaurants
		Other services

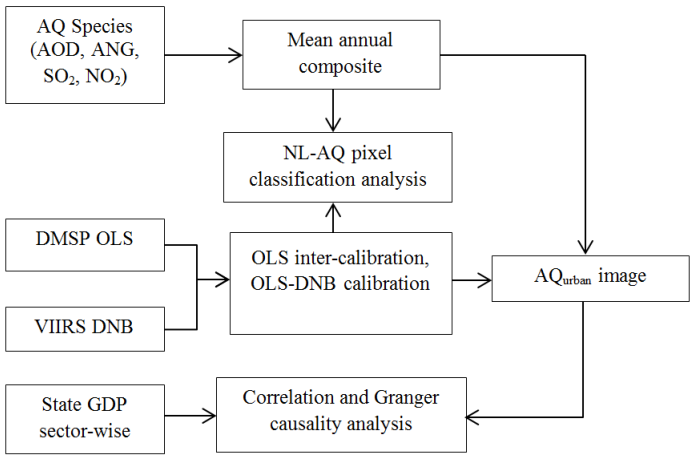

Figure 2: Flowchart of study outlining data sources, processing and analysis.

2.3 Data processing

2.3.1 Mean annual AQ composite

Each of the AQ species, i.e. ANG, AOD, SO_2 and NO_2 daily level retrievals were composited to mean annual images since timescale of other datasets employed is also annual. Instead of simply averaging daily images to annual scale, mean of 2%ile to 98%ile intensity values for each pixel was considered to remove effect of high outliers (due to surface reflectance) and zero values (due to cloud mask).

AOD daily values from MODIS dataset (AOD_{MOD}) were assessed also for accuracy by comparing the daily data with observations from AERONET (AOD_{AER}) ground stations. MODIS sensor is aboard Terra satellite whose revisit times are daily at 1030 hours, therefore the pixel values were compared with mean of observations of AERONET data collected between 0930 to 1130 hours. Since AERONET does not measure AOD at the same wavelength as MODIS (=550nm), AERONET measurements were extrapolated from AOD measured at 500nm and 440nm to 550nm using the relation (Liu et al., 2004):

$$\alpha_{\lambda 1-\lambda 2} = -d\ln\tau_\lambda / d\ln\lambda = -\ln(\tau_{\lambda 1}/\tau_{\lambda 2})/\ln(\lambda 1/\lambda 2) \quad (1)$$

where $\tau_{\lambda 1}$ and $\tau_{\lambda 2}$ are AOD values at wavelengths $\lambda 1$ and $\lambda 2$.

2.3.2 NL inter-calibration

OLS inter-calibration:In addition to the OLS dataset consisting of annual composites from different satellite sensors (F16 and F18 satellites), the sensors suffer pixel saturation in urban regions and themselves undergo physical degradation over a period of time. To overcome these deficiencies and ensure a continuous dataseries, the NL images were inter-calibrated using the invariant region method (Wu et al., 2013) by taking the year 2006 as base year. The calibration technique follows a power law function $DN_c + 1 = a \times (DN_m + 1)^b$, where DN_c is the grey value DN obtained post-calibration, DN_m is the grey value pre-calibration DN, and a and b are model coefficients as mentioned in the

paper by Wu et al. (2013).

OLS & DNB inter-calibration: Since OLS datasets are not available post year 2013, to enable continuity of NL dataset until 2014, F182013 OLS image was calibrated with January 2013 BETA monthly DNB composite. Using the conversion formula (Doll, 2008) first radiance (rad_{DN}) was calculated from DN :

$$rad_{DN} = (DN)^{3/2} Watts/cm^2/sr \tag{2}$$

After resampling the DNB image to the resolution of OLS,lookup-table of mean rad_{DNB} for rad_{DNB} values for each pixel coordinate was prepared. Due to the limitation of OLS sensor to measure only 64 levels, each level of DN had multiple differing DNB physical radiance values (rad_{DNB}). For calibration, mean rad_{DNB} was linearly regressed with corresponding rad_{DN} values. Linear regression is preferred since radiance from OLS and DNB represent the same physical measurement yet due to oversaturation of pixels in OLS, fitting an exponential curve was also explored, as discussed in later in Section 2.5.2.

2.4 Analysis

2.4.1 Trend of pixel classification by NL and AQ

Using nighttime light data, which correlate well with economic activities, and air quality species data observed from satellite, the authors have previously devised a scheme of classifying regions (Misra and Takeuchi, 2016) into LowLight-HighPollution (LLHP), HighLight-HighPollution (HLHP), LowLight-LowPollution (LLLP) and HighLight-LowPollution (HLLP), as per their AQ levels and NL intensity. In this research the classification scheme was applied on a time series nightlight data to draw inferences about transitions of pixel from one class to another. Based on inferences from classification trends, relationship between various economic activities (such as construction, manufacturing, vehicle population etc.) and air quality species is explored. Trend results derived were then used with causality results found in Section 2.4.2.

2.4.2 Correlation and Granger causality between AQ and GDP

To analyze the impact of economic activities on urban air quality both correlation and Granger causality tests (Granger, 1988) were performed between AQ species and each of the GDP sectors. For this, firstly image showing AQ levels for only urban regions was generated from which state level total values for each AQ species was calculated and compared with the state GDP of different economic sectors (GDP_{sec}).

To generate AQ images for urban regions, first a binary NL image for each year was prepared by considering only pixel locations with $DN >= 20$. It was found on visual inspection that by setting $DN >= 20$ urban areas and their peripheral regions could be distinguished from the non-urban regions. Binary NL image of each year also shows the growth of urban areas,hence signifying expansion of human activities. Thereafter corresponding years' binary NL images were multiplied by the mean annual AQ composites (as generated in Section 2.3.1; referred to as AQ_{mean} henceforth) to generate urban AQ images for each AQ species(referred to as AQ_{urban} hence).

For each state, correlation was computed between the state level total values for each of the AQ species and GDP_{sec} to find how each economic sector is related to individual AQ species. Further for each state these correlations were calculated for two region types: (a)only urban regions , (b) only non-urban regions. That is, correlation of GDP_{sec} was found both with AQ_{urban} as well as $AQ_{nonurban}$ (which is the difference of AQ_{mean} and AQ_{urban}). The reason for doing so was to identify which economic sectors are strictly an urban phenomena and could be contributing to urban air pollution directly or indirectly. Thus it was assumed that for such sectors $correlation(AQ_{urban}, GDP_{sec})$ shall be higher than other sectors as well as $correlation(AQ_{urban}, GDP_{sec}) >> correlation(AQ_{nonurban}, GDP_{sec})$.

However despite compliance with stated assumptions one still cannot say with statistical confidence if a particular sector 'causes' pollution. To overcome this weakness, Granger causality test (GCT) was employed. To identify the cause and effect in a causality relationship, GCT works on the principle that: 'the cause occurs before the effect' and 'the causal series contains special information about the series being caused that is not available in the other available series' (Granger, 1988). Each pair of GDP_{sec} and AQ_{urban} is tested as bivariate function with lags to find out if economic growth of the sector causes change in a AQ species levels or whether change in a AQ species levels causes economic growth of the sector. Since GCT is a time-series model based test, first the dataseries is checked if stationarity criteria at 90% confidence interval is satisfied using the Augmented Dicky-Fuller (ADF) unit root test (MacKinnon, 2010) . If a unit-root is found, it was removed by differencing once or twice or taking a rolling mean of the dataseries. GCT was subsequently performed for each cause-effect pair both forwards and backwards and the

Station	Observation count	Slope	R^2
Kanpur	2280	1.10	0.80
Pune	1320	0.95	0.79
Lahore	1238	0.90	0.77
Jaipur	1181	1.03	0.75
Karachi	1171	0.62	0.71
Gandhi College	877	1.11	0.72
Dhaka University	400	0.94	0.70
Kathmandu-Bode	335	0.81	0.89
Bhola	300	1.13	0.73
Nainital	284	0.95	0.65
Pantnagar	280	0.85	0.85

Table 2: Parameters of best-fit line obtained between AOD_{MOD} and AOD_{AER}

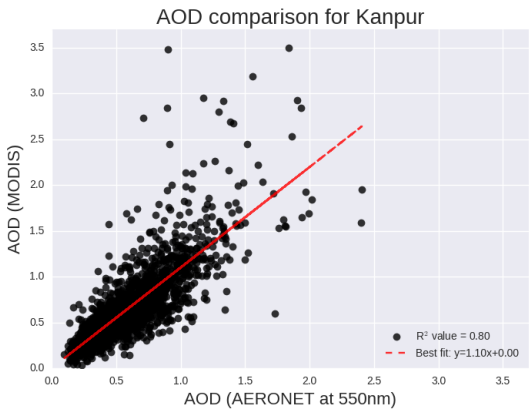

Figure 3: Calibration for Kanpur station

direction of causality was ascertained only if $p < 0.05$ condition for both 'likelihood ratio test' and 'chi-square test' was satisfied. Both the ADF and GCT were implemented using the 'StatsModel' module for Python2.7.

2.5 Results and discussion

2.5.1 Comparison of AOD_{MOD} and AOD_{AER}

The results of correlation between AOD_{MOD} and AOD_{AER} show good agreement as can be seen by the generally good values of R^2(greater than 0.70) and the slope of fit almost equable to unity in most cases. All results are presented in Table 2. It was also seen that for higher AOD_{AER} values, AOD_{MOD} tended to overestimate as can bee seen from Figure 3

2.5.2 OLS & DNB intercalibration

OLS data suffers from oversaturation in urban areas and this is evident while calibration with DNB. Until DN = 53 a linear trend line was fitted and thereafter an exponential curve is fitted to account for sudden increase in corresponding DNB values. For the linear fit, intercept was constrained to zero to ensure rad_{DNB} is always zero when rad_{DN} is zero. The piecewise calibration function finally adjudged was:

$$rad_{DNB} = \begin{cases} 0.02 rad_{DN} & DN \leq 53 \\ 7.34 \times 10^{-8} e^{0.04 rad_{DN}} + 9.61 & DN > 53 \end{cases} \quad (3)$$

R^2 for the piece-wise trend was found to 0.89. Even though it appears to be quite high, error bars of standard deviation of rad_{DNB} associated with each rad_{DN} are quite large as seen in Figure 4a. It points to the inadequacy of Equation 3 to accurately represent measured rad_{DNB} specially for pixels with higher intensities.

2.5.3 Correlation of NL and GDP

Several researches have found good correlation between total NL (TNL) and GDP for India as well as other countries ((Bhandari and Roychowdhury, 2011, Forbes, 2013, Sutton et al., 2007)). However this is the first research to use time-series inter-calibrated OLS data to compare it with GDP of India at both country and district scales. This enables to ascertain if the calibrated NL can be used as an indicator of economic activities in 2.4.1.At the country scale correlation between TNL and per capita GDP for the years 2001 to 2013 was found as 0.89. Using 'spatial analytic approach'by considering region wise NL, urban population and sub-national GDP of India previously Sutton et al. (2007) found a correlation of 0.84 for the year 2000 data. Thus NL can capture macroeconomic trends at both sub-national and temporal scale. However when the TNL at district level was compared to its GDP an interesting feature was found. Districts with low GDP (around INR 40 billion) were generally better correlated with TNL than districts having higher GDP (around INR 160 billion). An extreme example of low and high GDP cities is shown in Figure 5. This can be a result of either weak inter-calibration of OLS images (disadvantaged by saturated light in high GDP regions) or the fact that TNL cannot adequately represent all activities going in high GDP regions very well. In other words there are other GDP generating economic activities taking place in high GDP regions which may not always translate into NL.

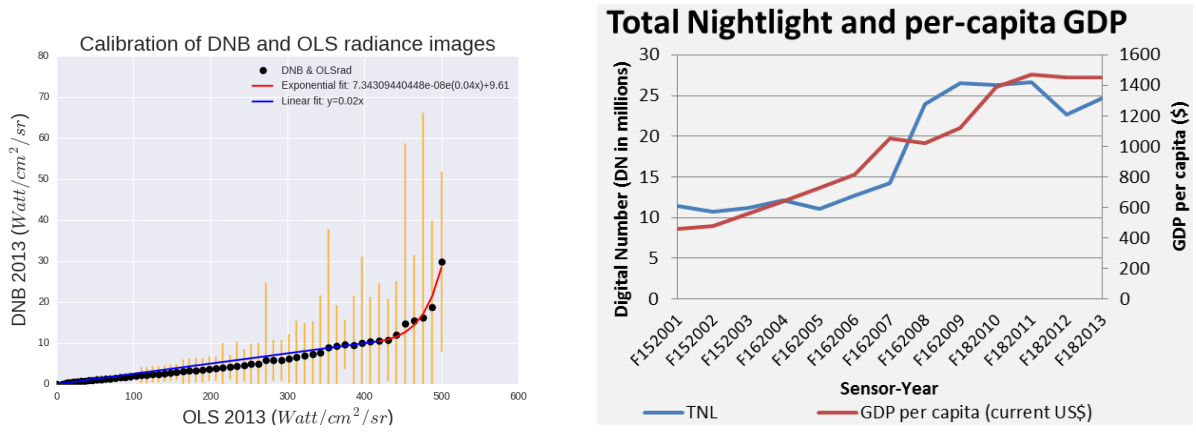

(a) (b)

Figure 4: (a) Calibration of DNB and OLS images for year 2013. Orange vertical lines represent error bar for that point; (b) Correaltion of Total Nightlight (TNL) and GDP was found to 0.89

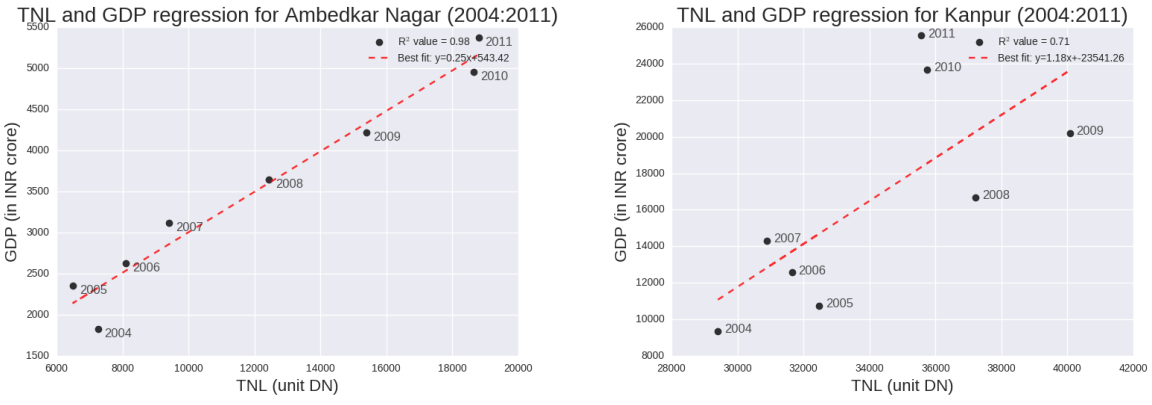

(a) (b)

Figure 5: (a)Ambedkar Nagar, a city with low GDP has R^2 of 0.98 (b) Kanpur, a city with high GDP has R^2 of 0.42

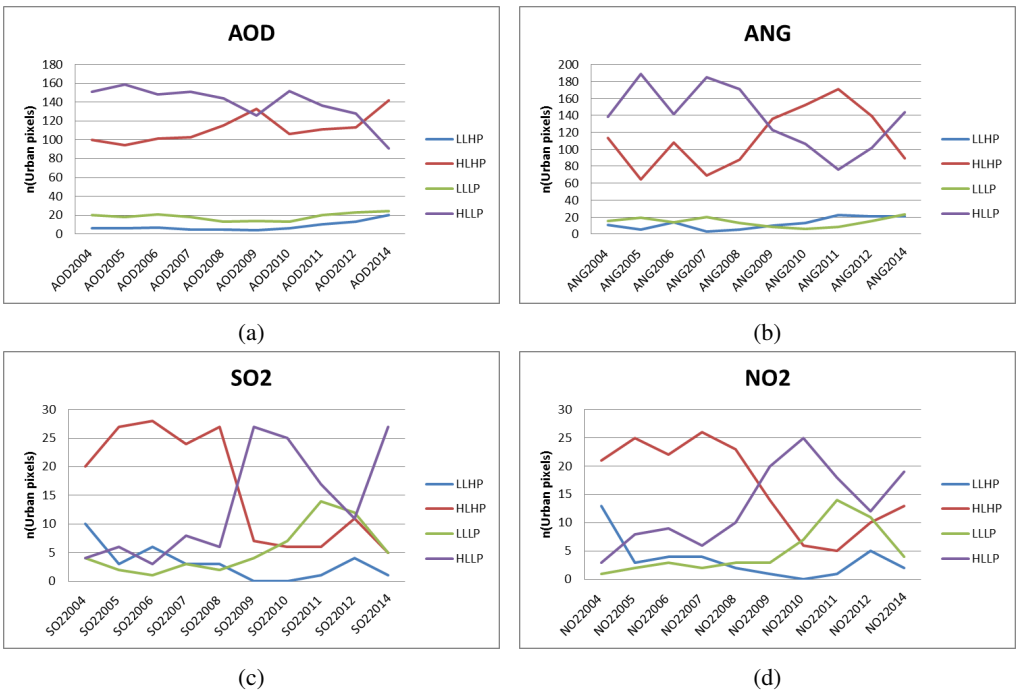

Figure 6: Time series count of urban pixels in each LLHP, HLHP, LLLP and HLLP class based on their NL values and (a) ANG values (b) AOD values (c) SO_2 values (d) NO_2 values

2.5.4 Trend of pixel classification by AQ and NL

For AOD, number of HLHP regions have increased since 2011 while for ANG, HLHP regions have decreased implying greater contribution of activities involving large aerosols (mineral dust) such as building-infrastructure construction in high economic activity areas. For SO_2 and NO_2 traditionally high economic regions have had high levels but in recent years while the number of such regions with high SO_2 has dwindled, for NO_2 the number decreased until 2010 but has increased back since. Following Bhanarkar et al. (2005) study of the Jameshedpur city about contribution of domestic household, industrial and vehicular emissions to urban SO_2 and NO_2, it can be assumed that decrease in SO_2 is on account of cleaner domestic fuel usage amongst other factors. However it is hard to say whether it is industrial or vehicular emissions that are bringing about change in NO_2. LLHP are cities in which the pollution due to economic activities is not well correlated with their night light. small cities may not have all their economic activities well correlated with NL: so even if light is low their pollution can be high. Steady increase in count of LLHP regions w.r.t ANG and AOD could indicate greater construction activities and biomass burning in smaller towns.

2.5.5 Correlation and Granger causality between AQ and GDP

The correlation analysis was performed on AQ_{urban} images (e.g. Figure 7a) as well as $AQ_{non-urban}$ images. For 4 states, urban regions as large as the minimum resolution of OMI images (i.e. 25km) could not be found so they were not considered for SO_2 and NO_2 analysis. From the correlation plots for each state, for example Figure 7b, it was seen that correlations of SO_2 with GDP_{sec} were generally much lower than that of AOD, ANG and NO_2. Yet the relative order of the correlation magnitude amongst sectors was found similar irrespective of the AQ species. Also almost all states had negative correlation of SO_2 for non-urban regions. For urban regions too SO_2 correlation was often negative in case of states with clean air quality but rose to high values for highly industrialized states like Gujarat and Tamil Nadu. Non-urban regions in most states (20 out of the 27) showed higher correlation of NO_2 with GDP_{sec} compared with urban regions. Thus, suggesting that sufficient anthropogenic sources of NO_2 are located outside defined urban regions. Generally for all AQ species the following GDP_{sec} were found to satisfy assumptions mentioned in Section 2.4.2: Registered Manufacturing, Unregistered Manufacturing, Construction, Industry, Railways, Communication and Public Administration.

By performing GCT test, 3 main causality scenarios were identified: (a) AQ species Granger causing sector GDP, (b) sector GDP Granger causing AQ species and (c) bidirectional Granger causality relationship between AQ species and sector GDP. Importantly for a fair number of the states (about 40%) Banking/Insurance, Construction and Industry sectors Granger caused AOD, ANG, SO_2 as well as NO_2. Further it was found that states which showed Granger causality from Industry sector to AQ species also shared the same relationship for the Construction sector. Also the

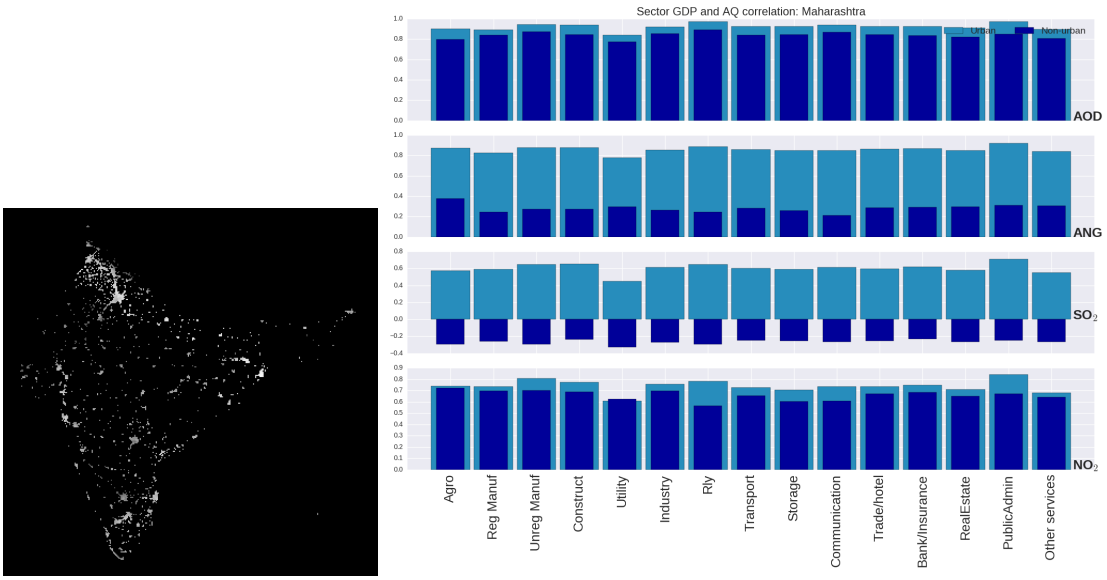

(a) (b)

Figure 7: (a) AOD_{urban} for the year 2010; (b) Correlation of different GDP sectors with each AQ species for Maharashtra state. Light blue represents correlation values for urban regions while dark represents the same for non-urban regions

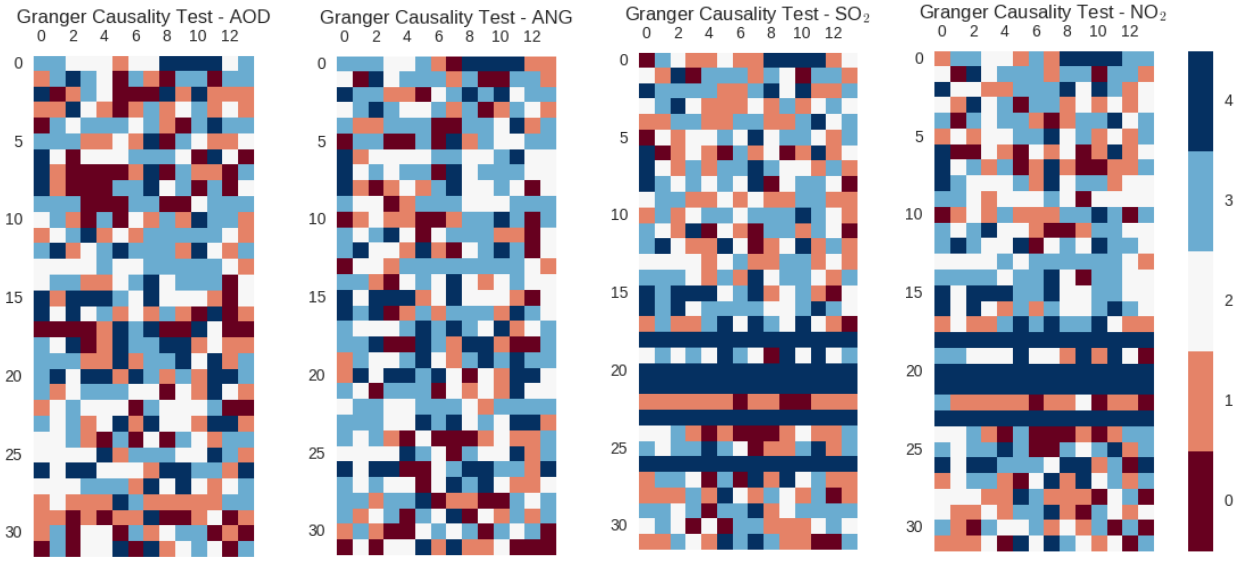

Figure 8: Granger causality test results of AOD, ANG, SO_2 and NO_2 with each GDP for sector for each state.*Vertical axis* on left side represents state AQ species: 0 - Andaman and Nicobar, 1- Andhra Pradesh, 2 - Arunachal Pradesh, 3 - Assam, 4 - Bihar, 5 - Chandigarh, 6 - Chhattisgarh, 7 - Delhi, 8 - Goa, 9 - Gujarat, 10- Haryana, 11- Himachal Pradesh, 12- Jammu and Kashmir, 13- Jharkhand, 14- Karnataka, 15- Kerala, 16 - Madhya Pradesh, 17 - Maharashtra, 18- Manipur, 19 - Meghalaya, 20 - Mizoram, 21 - Nagaland, 22 - Orissa, 23 - Puducherry, 24 - Punjab, 25 - Rajasthan, 26 - Sikkim, 27 - Tamil Nadu, 28 - Tripura, 29 - Uttar Pradesh, 30 - Uttaranchal, 31 - West Bengal; *Horizontal axis* for each AQ species represents the GDP sector: 0 - Agriculture and allied, 1 - Bank &Insurance , 2 - Communication , 3 - Construction, 4 - Industry, 5 - Other services 6 - Public Administration, 7 - Real Estate, 8 - Registered Manufacturing, 9 - Railways, 10 - Trade, hotel & restaurants, 11 - Transport, 12 - Unregistered Manufacturing, 13 - Electricity, water & gas; *Legend on right* represents the direction of causality: 0 - No causal relationship found, 1 - AQ species Granger causes sector GDP, 2 - Sector GDP Granger causes AQ species, 3 - Bidirectional relationship between AQ species and sector GDP, 4 - Data not stationary

states in which the Banking/Insurance sector Granger causes AOD, showed a similar relation with Construction sector a well. Considering a specific case example of Uttar Pradesh state, where 5 cities had the world's dirtiest air quality

in 2014 (World Health Organization, 2014), Granger causes were found as shown in Table 3.

Table 3: Structural composition of GDP in India by economic sectors.

AQ species	Granger cause
AOD	Transport
ANG	Communication, Public Administration , Railways
SO_2	Communication, Railways
NO_2	Agriculture, Construction, Transport, Electricity water and gas

How the other two directions of Granger causality, namely backward and bidirectional, are related with air quality is not discussed here as they are out of scope of this paper. One another approach could be determine sectors responsible for AQ species could be to first find interdependence between the sectors themselves to understand their effect in greater clarity.

As a note of caution Granger causality is not necessarily true causality. If a particular pair of sector GDP and AQ species is controlled by a common third process even then the GCT test may show fail to reject the alternative hypothesis of Granger causality. Yet, with the obtained results more research efforts can be directed into examining causality in detail. Also, with the causality map policy making for any state can be enabled for economic domains identified as cause. Regions can also be clustered for policy intervention based on common NL and AQ classification trends and Granger causality relationships. It is expected that regions with lesser economic activities are likely to show higher rates of air quality degradation under economic growth. This analysis can be used to develop an index to track an urban region's air quality trend with respect to its economic activities. Such an index will be useful to estimate associated effect on public health due to urban air pollution arising out of economic activities.

2.6 Conclusion

In this paper multi-year OLS and DNB datasets were calibrated to result in a time series night light data which was found suitable to represent GDP at country and district scales. Amongst the AQ datasets used, AOD from MODIS was assessed for accuracy and was found to have a good enough correlation with ground AOD from several AERONET stations. By studying trend of pixel classified by AQ and NL, it was deduced that infrastructure building are leading to buildup of mineral dusts in areas with high economic activity. In the final section by assessing correlation between various state level macroeconomic GDP indicators and air quality over 2004 to 2014 years a correlation and Granger causality plot was prepared. Using these plots finding whether growth in a specific economic sector shall cause increase in urban pollutants becomes clear. Importantly for 40% states Banking/Insurance, Construction and Industry sectors were identified to Granger cause AOD, ANG, SO_2 as well as NO_2. These results can directly be incorporated in policy studies to assess detailed mechanism of their effects. We also suggest using higher resolution economic data at district scale to study the impact of economic activities on urban air quality in more detail.

Acknowledgements

We thank the AERONET teams, especially Dr S.N. Tripathi and Dr. Brent Holben.

References

Baugh, K., Hsu, F.-C., Elvidge, C. D., and Zhizhin, M. (2013). Nighttime Lights Compositing Using the VIIRS Day-Night Band: Preliminary Results. *Proceedings of the Asia-Pacific Advanced Network*, 35:70.

Bhanarkar, A., Goyal, S., Sivacoumar, R., and Chalapattirao, C. (2005). Assessment of contribution of SO2 and NO2 from different sources in Jamshedpur region, India. *Atmospheric Environment*, 39(40):7745–7760.

Bhandari, L. and Roychowdhury, K. (2011). Night Lights and Economic Activity in India: A study using DMSP-OLS night time images. *Proceedings of the Asia-Pacific Advanced Network*, 32:218.

Central Statistic Office (2012). National Accounts Statistics - Sources and Methods, 2012. Technical report, Ministry of Statistics and Programme Implementation, Government of India, New Delhi.

Doll, C. N. H. (2008). CIESIN Thematic Guide to Night-time Light Remote Sensing and its Applications. *Earth Science*, pages 1–41.

Elvidge, C. D., Ziskin, D., Baugh, K. E., Tuttle, B. T., Ghosh, T., Pack, D. W., Erwin, E. H., and Zhizhin, M. (2009). A fifteen year record of global natural gas flaring derived from satellite data. *Energies*, 2(3):595–622.

Forbes, D. J. (2013). Multi-scale analysis of the relationship between economic statistics and DMSP-OLS night light images. *GIScience & Remote Sensing*, 50(5):483–499.

Fujikawa, A. and Takeuchi, W. (2013). Characterization of air quality in global mega- cities by OMI and MODIS measurements. In *34th Asian conference on remote sensing (ACRS)*, Bali, Indonesia.

Granger, C. (1988). Some recent development in a concept of causality. *Journal of Econometrics*, 39(1-2):199–211.

Holben, B., Eck, T., Slutsker, I., Tanré, D., Buis, J., Setzer, A., Vermote, E., Reagan, J., Kaufman, Y., Nakajima, T., Lavenu, F., Jankowiak, I., and Smirnov, A. (1998). AERONET - A Federated Instrument Network and Data Archive for Aerosol Characterization. *Remote Sensing of Environment*, 66(1):1–16.

Kanjilal, K. and Ghosh, S. (2013). Environmental Kuznet's curve for India: Evidence from tests for cointegration with unknown structuralbreaks. *Energy Policy*, 56:509–515.

Katayama, N. and Takeuchi, W. (2014). Comparison between Nighttime Light and Socioeconomic Indicators an an International Scale Using VIIRS Day-Night Band. In *35th Asian Conference of Remote Sensing*, Nay Pyi Taw.

Liu, Y., Sarnat, J. A., Coull, B. A., Koutrakis, P., and Jacob, D. J. (2004). Validation of Multiangle Imaging Spectroradiometer (MISR) aerosol optical thickness measurements using Aerosol Robotic Network (AERONET) observations over the contiguous United States. 109:1–9.

MacKinnon, J. G. (2010). *Critical values for cointegration tests*. PhD thesis, Queen's University, Department of Economics.

Managi, S. and Jena, P. R. (2008). Environmental productivity and Kuznets curve in India. *Ecological Economics*, 65(2):432–440.

Misra, P. and Takeuchi, W. (2015). Analysis of Air Quality in Indian Cities using Remote Sensing and Economic Growth Parameters. In *36th Asian Conference of Remote Sensing*, Manila.

Misra, P. and Takeuchi, W. (2016). Analysis of air quality and nighttime light for Indian urban regions. *IOP Conference Series: Earth and Environmental Science*, 37:012077.

Sutton, P., Elvidge, C., and Ghosh, T. (2007). Estimation of gross domestic product at sub-national scales using nighttime satellite imagery. *International Journal of Ecological Economics & Statistics*, 8(S07):5–21.

World Health Organization (2014). Ambient (outdoor) air pollution in cities database 2014.

Wu, J., He, S., Peng, J., Li, W., and Zhong, X. (2013). Intercalibration of DMSP-OLS night-time light data by the invariant region method. *International Journal of Remote Sensing*, 34(20):7356–7368.